Journal of Nuclear Materials 409 (2011) 9–17

Contents lists available at ScienceDirect

Journal of Nuclear Materials

journal homepage: www.elsevier.com/locate/jnucmat

Phase study in Sr–Th–P–O system: Structural and thermal investigations of quaternary compounds

Meera Keskar *, Rohan Phatak, S.K. Sali, K. Krishnan, N.D. Dahale, N.K. Kulkarni, S. Kannan

Fuel Chemistry Division, Bhabha Atomic Research Centre, Trombay, Mumbai 400 085, India

ARTICLE INFO

Article history:
Received 23 September 2010
Accepted 3 December 2010
Available online 15 December 2010

ABSTRACT

The sub-solidus phase relations in Sr–Th–P–O quaternary system were determined at 1223 K in air. To confirm the formation and stability of reported phases, ternary and quaternary compounds in Sr–Th–O, Sr–P–O, Th–P–O and Sr–Th–P–O systems were synthesized by solid state reactions of $SrCO_3$, ThO_2 and $NH_4H_2PO_4$ in desired molar proportions at 1223 K. A pseudo-ternary phase diagram of $SrO–ThO_2–P_2O_5$ system was drawn on the basis of the phase analysis of various phase mixtures and phase fields were established by powder X-ray diffraction. In the phase diagram, three quaternary compounds $SrTh(PO_4)_2$, $SrTh_4(PO_4)_6$ and $Sr_7Th(PO_4)_6$ were identified. When heated in air at 1673 K, these compounds decompose to ThO_2. Structures of $SrTh(PO_4)_2$, $SrTh_4(PO_4)_6$ and $Sr_7Th(PO_4)_6$ were derived from X-ray powder data using the Rietveld refinement method. Thermal expansion behaviors of $SrTh(PO_4)_2$, $SrTh_4(PO_4)_6$ and $Sr_7Th(PO_4)_6$ were investigated using high-temperature X-ray diffraction in the temperature range of 298–1273 K.

1. Introduction

Considering the large thorium reserves available in India, thoria based nuclear fuels have attracted a great interest for the future nuclear energy program. It is proposed to use $(Th,U)O_2$ or $(Th,Pu)O_2$ containing 4–6% of uranium or plutonium dioxides (as a fissile materials), as fuel materials for the advance heavy water reactors or fast breeder reactors [1].

The minor actinides and fission products obtained during reprocessing of spent nuclear fuels from these reactors can be effectively managed by immobilizing these highly radioactive and long-lived isotopes in stable and suitable matrices. A vast variety of studies have been reported for the search of suitable host matrices as an alternate to borosilicate glass for the immobilization of highly radioactive minor actinides and fission products. Many workers have reported that the phosphate matrices such as: appatites $[(Ca_{10}PO_4)_6X_2]$ [2], monazites $[M^{III}PO_4]$ [3,4], cheralite $[M^{II}M^{IV}(PO_4)_2]$ [5–7], zirconium phosphate $[Zr_2O(PO_4)_2]$ [8], NZP $[NaZr_2(PO_4)_3]$ [9], thorium phosphate di-phosphate [10], lead phosphate [11] and iron phosphate [12] have the potential to be used as host matrices for the immobilization. Among them, thorium phosphate-di-phosphate [β-TPD] and thorium di-phosphate $[ThP_2O_7]$, in ceramic form with qualities such as; high resistance to water corrosion and radiation damage, high thermal and chemical stability, low thermal expansion and very low leachability appear as alternative host matrices [10,13–19]. TPD can be prepared either by wet or dry chemical routes [10,20], whereas pure ThP_2O_7 can be prepared only by solution route [21]. TPD shows possibility to substitute Th^{4+} with smaller cations such as; U^{4+}, Np^{4+} and Pu^{4+} (up to 75, 52 and 41 mol%, respectively) [13,15,21–23]. The chemistry of both trivalent and tetravalent actinide phosphates have been recently re-examined in detail [24–26]. Brandel et al. [27] have suggested that TPD can be used to incorporate mono, di and trivalent cations. Krishnan et al. [28] have recently reported the structures of alkali metal thorium phosphates and studied their thermal expansion characteristics using HT-XRD. Guesdon et al. [29] have reported several thorium phosphates and showed great flexibility in their structures to accommodate other ions.

Strontium is one of the important long lived fission products (^{90}Sr, $T_{1/2}$ = 28.5y) formed during the nuclear fission reaction. It is of interest to explore the possibility of incorporating Sr in TPD or thorium di-phosphate matrix. Therefore it is necessary to know the chemistry of various phases in $SrO–ThO_2–P_2O_5$ system and also co-existence of these phases. In $SrO–ThO_2$ system, $SrThO_3$ is the only compound reported so far and its thermal expansion was investigated using dilatometry [30]. The synthesis and characterization of various phosphates of thorium are reported by Bamberger et al. [31]. Sarawadekar and Kulkarni [32] have studied the structural and thermal properties of various alkaline earth metal ortho-phosphates using XRD, TG/DTA and IR techniques.

The structures of various metal thorium phosphates are discussed in detail by Locock [33]. In Sr–Th–P–O quaternary system, three quaternary compounds $SrTh(PO_4)_2$, $SrTh_4(PO_4)_6$ and $Sr_7Th(PO_4)_6$ are reported which were synthesized by solid state reactions of $SrCO_3$, ThO_2 and $NH_4H_2PO_4$ at 1473 K [27,29,34,35].

* Corresponding author. Tel.: +91 22 25590643; fax: +91 22 25505151.
E-mail address: meerakeskar@yahoo.com (M. Keskar).

0022-3115/$ - see front matter © 2010 Elsevier B.V. All rights reserved.
doi:10.1016/j.jnucmat.2010.12.014

However, their structural and thermal studies have not been reported. The structural investigations of cheralite (initially called brabantite) like compounds of type $M^{II}An^{IV}(PO_4)_2$ (M^{II} = Ca, Cd, Sr, Pb and An^{IV} = Th, U, Np) are reported [36–39]. The structures of cheralite type phosphates consist of $M^{II}(An)O_9$ nine vertex polyhedron and PO_4 tetrahedra linked by oxygen atoms into three-dimensional network. The polyhedra share edges to form chains that extend in the b direction and linked in the c direction by the PO_4 tetrahedra. $SrTh_4(PO_4)_6$ compound is related to $M^{I}Th_2(PO_4)_3$ type of structure which has a flexibility towards substitution of M^{I} by M^{II} and Th by other tetravalent actinide ions [29].

In this communication we report extensive studies on the synthesis and characterization of various ternary and quaternary phases in $SrO–ThO_2$, $SrO–P_2O_5$ and $ThO_2–P_2O_5$ systems. The information obtained was further used to draw the pseudo-ternary phase diagram of Sr–Th–P–O system at 1223 K. Structural studies of $SrTh(PO_4)_2$, $SrTh_4(PO_4)_6$ and $Sr_7Th(PO_4)_6$ were carried out by Rietveld analysis of powder X-ray data. The thermal expansion behaviors of these compounds were also investigated by high-temperature X-ray diffraction technique.

2. Experimental

2.1. Synthesis of samples

All the ternary and quaternary phases in $SrO–ThO_2$, $SrO–P_2O_5$, $ThO_2–P_2O_5$ and $SrO–ThO_2–P_2O_5$ systems were synthesized by solid state route. Ammonium di-hydrogen ortho-phosphate ($NH_4H_2PO_4$), $SrCO_3$ (both analar grade, Merck, 99.99% purity) and ThO_2 were used as starting materials. ThO_2 was obtained by decomposition of thorium oxalate at 1073 K in air. All three reactants were mixed in different molar proportions for making equilibrium phase mixtures as listed in Table 1. The mixtures were heated in a resistance heating furnace in an alumina boat at 673 K for 6 h (to decompose $NH_4H_2PO_4$) followed by grinding and re-heating at 1223 K for 48 h in air.

2.2. Instrumental analysis

X-ray diffraction patterns for all the compounds were recorded on STOE X-ray diffractometer (having θ–θ geometry) using graphite monochromatized Cu Kα1 radiation (λ = 0.15406 nm) at the scanning rate of 1°(2θ) min^{-1}. For the structural studies of $SrTh(PO_4)_2$, $SrTh_4(PO_4)_6$ and $Sr_7Th(PO_4)_6$, the diffraction patterns were recorded in the 2θ range of 10–100° with step size of 0.02°(2θ) and a counting time of 5 s per step. Simultaneous TG/DTA for the three quaternary compounds were recorded up to 1673 K on a Mettler Thermoanalyser (model: TGA/SDTA 851^e/MT5/LF1600). The samples were heated in alumina cups at the heating rate of 10 K/min in a flowing stream of dry air with a flow rate 50 ml/min. Thermoanalyser was calibrated using thermal decomposition of $CaC_2O_4·H_2O$ to CaO from 298 to 1273 K in air. HT-XRD data for $SrTh(PO_4)_2$, $SrTh_4(PO_4)_6$ and $Sr_7Th(PO_4)_6$ were recorded on STOE X-ray diffractometer using HDK-2.4 Buhler high-temperature attachment under vacuum (10^{-8} bar) in the temperature range of 298–1273 K. The silicon and platinum stage were used to calibrate the instrument. Further details on instrumentation about HT-XRD are given elsewhere [40].

3. Results and discussion

3.1. Phase diagram study

Three ternary systems $SrO–ThO_2$, $SrO–P_2O_5$ and $ThO_2–P_2O_5$ and one quaternary system Sr–Th–P–O were used for drawing the phase diagram. The "*d*" values of the reported ternary and quaternary compounds listed in ICDD cards were used for phase identification of heated products of nineteen phase mixtures, synthesized during the present work.

3.1.1. $SrO–ThO_2$ system

The presence of low density ternary oxide $SrThO_3$ formed during the interaction of fuel with fission products, may critically affect the properties of fuel materials and therefore various properties of $SrThO_3$, are studied by many workers. Subasri et al. [41] have reported that the SrO has limited solubility in thoria and not forming $SrThO_3$. On the other hand, $SrThO_3$ was successfully synthesized by a citrate–nitrate gel combustion technique by Purohit et al. [30] and its bulk thermal expansion was measured by dilatometry. Recently, Shein et al. [42] have studied the stability of $SrThO_3$ and remarked that the compound is unstable in comparison with a mechanical mixture of constituent binary oxides. Dharwadkar [43], during the determination of Gibbs free energy formation of $SrThO_3$ has stated that though the formation of compound is thermodynamically possible, the compound is marginally stable. Several attempts were made by us to synthesis $SrThO_3$

Table 1
Identification of various phases on heat treatment of different proportions of SrO, ThO_2 and P_2O_5 at 1223 K in air.

Mixture no.	Mole fraction of the oxides			Phases identified by XRD		
	SrO	ThO_2	P_2O_5			
1	0.33	0.33	0.34	$SrTh(PO_4)_2$ [A]		
2	0.13	0.5	0.37	$SrTh_4(PO_4)_6$ [B]		
3	0.64	0.09	0.37	$Sr_7Th(PO_4)_6$ [C]		
4	0.35	0.37	0.28	$SrTh(PO_4)_2$	ThO_2	$SrCO_3$
5	0.65	0.2	0.15	$SrTh(PO_4)_2$	ThO_2	$SrCO_3$
6	0.7	0.1	0.2	$SrTh(PO_4)_2$	$Sr_7Th(PO_4)_6$	$SrCO_3$
7	0.15	0.55	0.3	$SrTh(PO_4)_2$	$Sr_7Th(PO_4)_6$	ThO_2
8	0.45	0.25	0.3	$SrTh(PO_4)_2$	$Sr_7Th(PO_4)_6$	$SrCO_3$
9	0.05	0.52	0.43	$SrTh_4P_6O_{24}$	$Th_4P_6O_{23}$	ThP_2O_7
10	0.15	0.35	0.5	$SrTh(PO_4)_2$	ThP_2O_7	ThP_4O_{12}
11	0.8	0.02	0.18	$Sr_7Th(PO_4)_6$	$Sr_3P_2O_8$	$SrCO_3$
12	0.55	0.1	0.45	$SrTh(PO_4)_2$	$Sr_2P_2O_7$	$Sr_3P_4O_{13}$
13	0.65	0.05	0.3	$SrTh(PO_4)_2$	$Sr_2P_2O_7$	$Sr_3P_2O_8$
14	0.35	0.15	0.5	$SrTh(PO_4)_2$	$Sr_3P_4O_{13}$	P_2O_5
15	0.05	0.65	0.3	$SrTh_4(PO_4)_6$	$Th_4P_6O_{23}$	ThO_2
16	0.15	0.45	0.4	$SrTh(PO_4)_2$	$SrTh_4(PO_4)_6$	ThP_2O_7
17	0.1	0.2	0.7	$SrTh(PO_4)_2$	ThP_4O_{12}	P_2O_5
18	0.2	0.7	0.1	$SrTh(PO_4)_2$	ThO_2	$SrCO_3$
19	0.42	0.43	0.15	$SrTh(PO_4)_2$	ThO_2	$SrCO_3$

either by solid state or by citrate–nitrate gel route described by Purohit et al. [30] could not yield the desired product. Hence, $SrThO_3$ was not included in this study for drawing the phase diagram.

3.1.2. ThO_2–P_2O_5 system

This pseudo-binary system has five established compounds, ThP_2O_7, ThP_4O_{12}, $Th_3P_2O_{11}$, $Th_3P_4O_{16}$ and $Th_4P_6O_{23}$ and are made up of ThO_2–P_2O_5 in the ratios of $(ThO_2)(P_2O_5)$, $(ThO_2)(P_2O_5)_2$, $(ThO_2)_3(P_2O_5)$, $(ThO_2)_3(P_2O_5)_2$ and $(ThO_2)_4(P_2O_5)_3$, respectively. Laud and Hummel [19], during the study of ThO_2–P_2O_5 system confirmed the existence of ThP_2O_7, $Th_3P_2O_{11}$ and $Th_3P_4O_{16}$. Cubic ThP_2O_7 is reported to be stable up to 1373 K and above 1523 K it decomposes to stable thorium phosphate-di-phosphate [21]. Though Clavier et al. [21] have reported that the solution route is the only route for the synthesis of pure ThP_2O_7 but we could synthesize pure ThP_2O_7 by solid state route. As the literature on actinide phosphate was rather limited and often controversial, the chemistry of thorium phosphates was completely re-examined by Clavier et al. [21] and Benard et al. [10]. During the present work, attempts were made to synthesize $Th_3P_2O_{11}$ and $Th_3P_4O_{16}$ by solid state route by heating the reactants in required proportions at 1223 K, but both the reaction products were identified as a mixture of TPD and ThO_2 and were not included in the phase diagram study. The existence of $Th_3P_4O_{16}$, synthesized by Bamberger et al. [31] was doubted by Brandel et al. [20], stating that either the phase is wrong or does not exist. A well established and most stable phase in ThO_2–P_2O_5 system, $Th_4(PO_4)_4(P_2O_7)$, is synthesized either by solid state or by solution route by heating the precursors at 1523 K [16,19]. Here, we could successfully synthesize pure

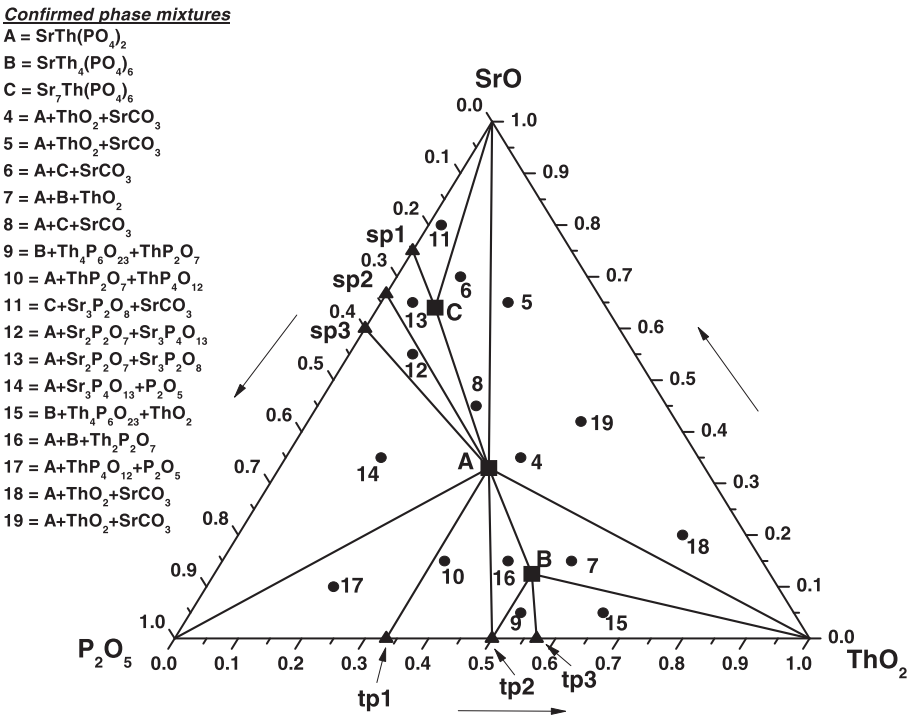

Fig. 1. Pseudo ternary phase diagram of SrO–ThO_2–P_2O_5 system drawn at 1223 K; sp1, sp2, sp3 refer strontium phosphates with compositions $Sr_3P_2O_8$, $Sr_2P_2O_7$, $Sr_3P_4O_{13}$, respectively and tp1, tp2, tp3 refer thorium phosphate with composition ThP_4O_{12}, ThP_2O_7 and $Th_4P_6O_{23}$, respectively.

Table 2
Crystallographic data for $SrTh(PO_4)_2$, $SrTh_4(PO_4)_6$ and $Sr_7Th(PO_4)_6$.

Compound	$SrTh(PO_4)_2$	$SrTh_4(PO_4)_6$	$Sr_7Th(PO_4)_6$
Radiation	Cu Kα1 λ = 0.15406 nm	Cu Kα1 λ = 0.15406 nm	Cu Kα1 λ = 0.15406 nm
Formula weight	509.6	792.8	1415.198
Model	$CaTh(PO_4)_2$	$NaTh_2(PO_4)_3$	$Ba_3La(PO_4)_3$
System	Monoclinic	Monoclinic	Cubic
Lattice parameters	a = 0.68011(2) nm	a = 1.74064(4) nm	a = 1.01874(1)
	b = 0.70229(2) nm	b = 0.68366(1) nm	
	c = 0.65143(2) nm	c = 0.81453(2) nm	
	β = 103.521(3)°	β = 101.181(2)°	
Space group	P21/n (no. 14)	C2/c (no. 15)	I-43d (no. 220)
V (nm)^3	0.30252(1)	0.950899(25)	1.05728(3)
Z	2	4	4
R_p (%)	6.20	5.53	8.21
R_{wp} (%)	7.04	6.47	10.78
R_F^2 (%)	9.84	7.07	12.32

$R_p = 100 \times \Sigma|y_{obs} - y_{cal}|/\Sigma|y_{obs}|$.
$R_{wp} = 100 \times \{[\Sigma w(y_{obs} - y_{cal})^2]/[(\Sigma w y_{obs})^2]\}^{1/2}$.
$R_F^2 = 100 \times \{[\Sigma(I_{obs} - I_{cal})]/[(\Sigma w y_{obs})^2]\}^{1/2}$.

thorium phosphate-di-phosphate (TPD) by heating the reactants for longer duration (45 h) at much lower temperature i.e. 1223 K. Thus during the present work, ThP_2O_7, ThP_4O_{12} and $Th_4P_6O_{23}$, phases were used for drawing the phase diagram at 1223 K.

3.1.3. $SrO–P_2O_5$ system

Alkaline earth phosphates, $M_3(PO_4)_2$ (M^{2+} = Mg, Ca, Sr, Ba) have been extensively studied in materials science due to the possibility of doping them with divalent or trivalent rare earth ions to produce efficient fluorescent materials [44]. In $SrO–P_2O_5$ system, SrP_2O_6, $Sr_2P_2O_7$, $Sr_3P_2O_8$, $Sr_4P_2O_9$, $Sr_2P_6O_{17}$ and $Sr_3P_4O_{13}$ compounds are reported and they are made up of $SrO–P_2O_5$ in the ratios of $(SrO)(P_2O_5)$, $(SrO)_2(P_2O_5)$, $(SrO)_3(P_2O_5)$, $(SrO)_4(P_2O_5)$, $(SrO)_2(P_2O_5)_3$ and $(SrO)_3(P_2O_5)_2$, respectively. The synthesis of α-SrP_2O_6 is reported by Hoppe [45], by heating the mixture of strontium carbonate and phosphorous acid at 1150 K in nitrogen atmosphere for 14 h. In order to confirm the formation of SrP_2O_6, $NH_4H_2PO_4$ and $SrCO_3$ were heated at 1223 K and the product was identified as a mixture of $Sr_3P_4O_{13}$, SrO and P_2O_5. Strontium di-phosphate, $Sr_2P_2O_7$ was synthesized by Brown and Calvo [46] by calcining the precursor obtained by solution route at 1473 K for 10 min. At 1223 K, we confirmed the formation of same by solid state route. Belik et al. [47] as well as Sarawadekar and Kulkarni [32] confirmed the existence of $Sr_3P_2O_8$ as a single phase, synthesized by both solid and solution routes by heating the precursors at 1173 K and 823 K, respectively. The formation of $Sr_3P_2O_8$ at 1223 K was confirmed by us during the present study. A single crystal study of $Sr_3P_4O_{13}$ was carried out by Zhang et al. [48], which was obtained by annealing Li_2CO_3, $SrCO_3$ and $NH_4H_2PO_4$ at 1073 K. We could also synthesize pure $Sr_3P_4O_{13}$ by solid state route at 1223 K. Though, $Sr_4P_2O_9$ and $Sr_2P_6O_{17}$ are reported in literature they are not well characterized and thus not included in the present phase diagram study. Thus in $SrO–P_2O_5$ system, three compounds $Sr_2P_2O_7$, $Sr_3P_2O_8$ and $Sr_3P_4O_{13}$ were used for drawing the phase diagram at 1223 K.

3.1.4. $SrO–ThO_2–P_2O_5$ system

In Sr–Th–P–O quaternary system, three quaternary compounds $SrTh(PO_4)_2$, $SrTh_4(PO_4)_6$ and $Sr_7Th(PO_4)_6$ are reported which were synthesized by solid state route by heating $SrCO_3$, ThO_2 and $NH_4H_2PO_4$ at 1473 K [29,34,35]. The former two phases belong to monoclinic system whereas the later belongs to cubic system [29]. In the present study, the formation of the same phases was confirmed at much lower temperature i.e. 1223 K and thus these phases were included in the phase diagram.

A pseudo-ternary phase diagram of $SrO–ThO_2–P_2O_5$ system is shown in Fig. 1 and was drawn on the basis of the phase analysis of the samples mixtures listed in Table 1, the knowledge of reported ternary phases in $SrO–ThO_2$, $SrO–P_2O_5$ and $ThO_2–P_2O_5$ ternary systems and three quaternary compounds $SrTh(PO_4)_2$, $SrTh_4(PO_4)_6$ and $Sr_7Th(PO_4)_6$, reported in Sr–Th–P–O quaternary system. The phases identified by XRD in the nineteen phase mixtures are listed in Table 1 along with their compositions. The compositions investigated by XRD analysis to establish the coexisting phases are shown as points and the respective stable phases are also indicated in Fig. 1. Phase boundaries were drawn on the basis of the reported ternary compounds. The compositions examined by XRD for phase-field determination are shown as circles, the pure quaternary compounds as squares and ternary compounds as triangles.

3.2. Structural study of $SrTh(PO_4)_2$, $SrTh_4(PO_4)_6$ and $Sr_7Th(PO_4)_6$

The XRD data of $SrTh(PO_4)_2$ and $SrTh_4(PO_4)_6$ recorded at 298 K were indexed on monoclinic system with refined lattice parameters $a = 0.6803(4)$ nm, $b = 0.7025(4)$ nm, $c = 0.6516(4)$ nm, $\beta = 103.517(3)^\circ$ and $a = 1.7410(6)$ nm, $b = 0.6838(2)$ nm, $c = 0.8148(3)$ nm, $\beta = 101.183(2)^\circ$, respectively. XRD data of $Sr_7Th(PO_4)_6$ recorded at room temperature was indexed on cubic system with lattice parameter $a = 1.0187(5)$ nm.

The Powder XRD patterns of $SrTh(PO_4)_2$, $SrTh_4(PO_4)_6$ and $Sr_7Th(PO_4)_6$ were used for structure refinement by Rietveld analysis using GSAS software [49] with the EXPGUI interface [50]. The lattice parameters and background was refined prior to refinement of the peak profile function and later atomic positions and thermal parameters were refined. Positional refinement of the lighter atoms (P and O) in presence of the high Z elements (Th and Sr)

Table 3
Refined position parameters, occupancies and isotopic displacement parameters for various atoms in $SrTh(PO_4)_2$, $SrTh_4(PO_4)_6$ and $Sr_7Th(PO_4)_6$.

Atom	x	y	z	Occ.	Uiso
$SrTh(PO_4)_2$					
Th	0.2164(8)	0.1610(9)	0.3989(4)	0.500	0.0322(7)
Sr	0.214(4)	0.161(4)	0.390(5)	0.500	0.028(2)
P	0.1997(21)	0.1613(20)	0.8892(24)	1.000	0.074(4)
O1	0.248(4)	0.4973(28)	0.447(4)	1.000	0.084(4)
O2	0.0267(27)	0.1089(31)	0.6969(26)	1.000	0.084(4)
O3	0.3659(30)	0.2092(32)	0.7711(34)	1.000	0.084(4)
O4	0.1187(26)	0.3291(27)	1.001(4)	1.000	0.084(4)
$SrTh_4(PO_4)_6$					
Sr	0.0218(9)	0.4212(31)	0.3576(16)	0.250	0.014(6)
Th	0.15311(12)	0.09299(28)	0.03630(25)	1.000	0.0133(2)
P1	0.3152(6)	0.0882(23)	0.3194(13)	1.000	0.01328(2)
P2	0.0000	−0.0870(33)	0.2500	1.000	0.01328(2)
O1	0.0645(12)	0.0684(29)	0.2564(32)	1.000	0.092(12)
O2	−0.0250(14)	−0.2300(25)	0.1030(26)	1.000	0.033(10)
O3	0.2300(8)	0.0388(30)	0.3308(25)	1.000	0.0215(80)
O4	0.3708(12)	−0.0891(27)	0.3337(24)	1.000	0.0282(60)
O5	0.2978(13)	0.1622(31)	0.1373(17)	1.000	0.0282(60)
O6	0.3514(15)	0.2504(26)	0.4419(25)	1.000	0.0133(2)
$Sr_7Th(PO_4)_6$					
Sr	0.0642(8)	0.0642(8)	0.0642(8)	0.875	0.055(1)
Th	0.0580(13)	0.0580(13)	0.0580(13)	0.125	0.055(1)
P	0.37500	0.0000	0.25000	1.000	0.025(3)
O	0.5557(20)	0.3632(10)	0.7016(20)	1.000	0.132(6)

Table 4
Interatomic distances (nm) in $SrTh(PO_4)_2$, $SrTh_4(PO_4)_6$ and $Sr_7Th(PO_4)_6$.

$SrTh(PO_4)_2$			
Th–O1	0.2385(19)	P–O1	0.1552(7)
Th–O1	0.2598(30)	P–O2	0.1549(7)
Th–O2	0.2590(22)	P–O3	0.1546(7)
Th–O2	0.2498(21)	P–O4	0.1551(7)
Th–O3	0.25374(25)		
Th–O3	0.2506(22)		
Th–O4	0.2790(27)		
Th–O4	0.2603(21)		
Th–O4	0.2661(18)		
$SrTh_4(PO_4)_6$			
Sr–O1	0.2700(26)	Th–O1	0.2586(23)
Sr–O1	0.2898(27)	Th–O1	0.2726(25)
Sr–O2	0.3161(22)	Th–O2	0.2481(25)
Sr–O2	0.2405(19)	Th–O3	0.2505(15)
Sr–O2	0.2646(24)	Th–O3	0.2537(20)
Sr–O4	0.2598(24)	Th–O4	0.2488(20)
Sr–O4	0.2657(25)	Th–O5	0.2538(21)
Sr–O4	0.3052(26)	Th–O5	0.2449(17)
$Sr_7Th(PO_4)_6$			
Sr–O	0.248063(2)	Th–O	0.246585(2)
Sr–O	0.248063(2)	Th–O	0.246585(2)
Sr–O	0.248063(2)	Th–O	0.246585(2)
Sr–O	0.249713(2)	Th–O	0.256883(2)
Sr–O	0.249713(2)	Th–O	0.256883(2)
Sr–O	0.249713(2)	Th–O	0.256883(2)
Sr–O	0.248063(2)	Th–O	0.246585(2)
Sr–O	0.248063(2)	Th–O	0.246585(2)

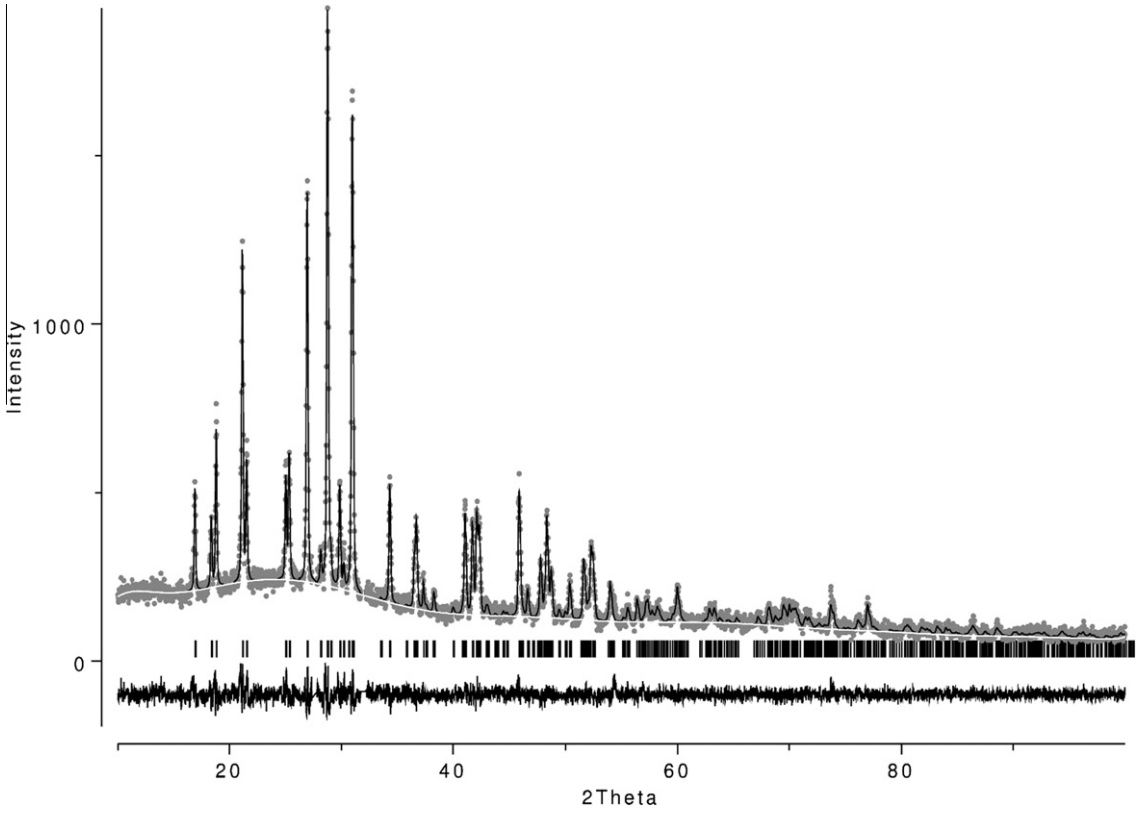

Fig. 2. Rietveld plot of observed and calculated diffraction pattern of $SrTh(PO_4)_2$.

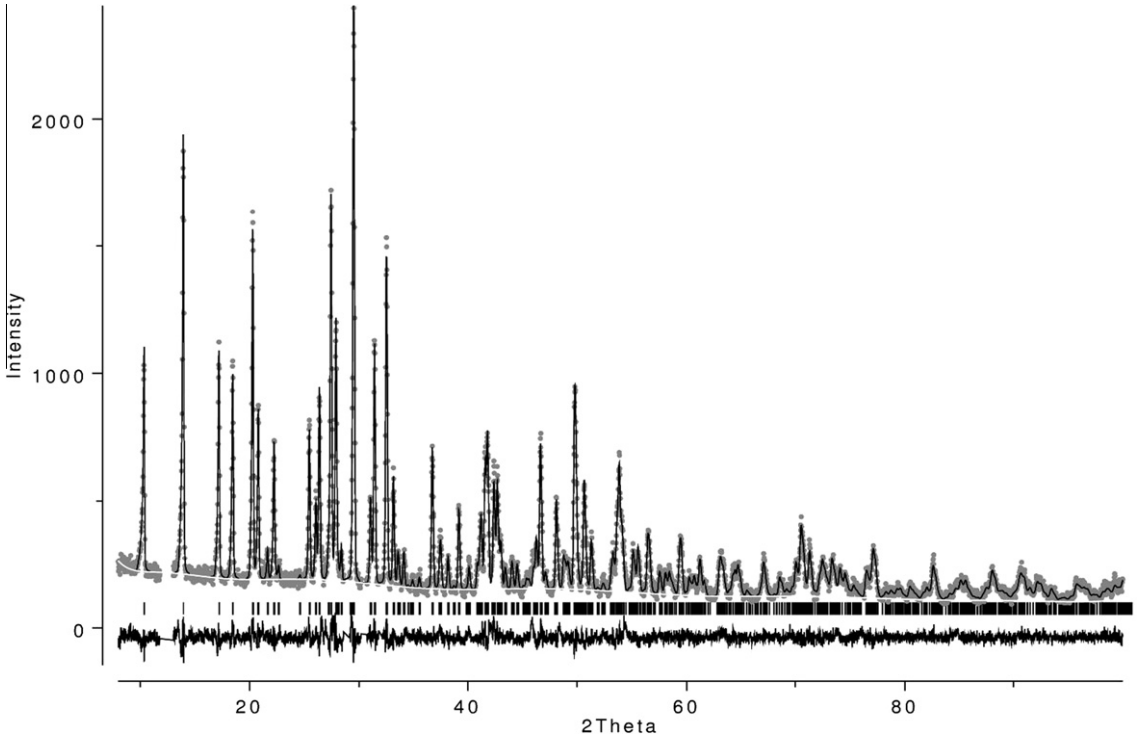

Fig. 3. Rietveld plot of observed and calculated diffraction pattern of $SrTh_4(PO_4)_6$.

was unstable leading to highly distorted P–O bond distances. Thus in the initial refinement cycles soft constraint of 0.154(3) nm was imposed on P–O bond distance with higher weighting factor equal to 20 and later reducing it to 1 in the final cycle. The refined crystal data of $SrTh(PO_4)_2$, $SrTh_4(PO_4)_6$ and $Sr_7Th(PO_4)_6$ are given in Table 2. The refined atomic parameters and the typical bond lengths for

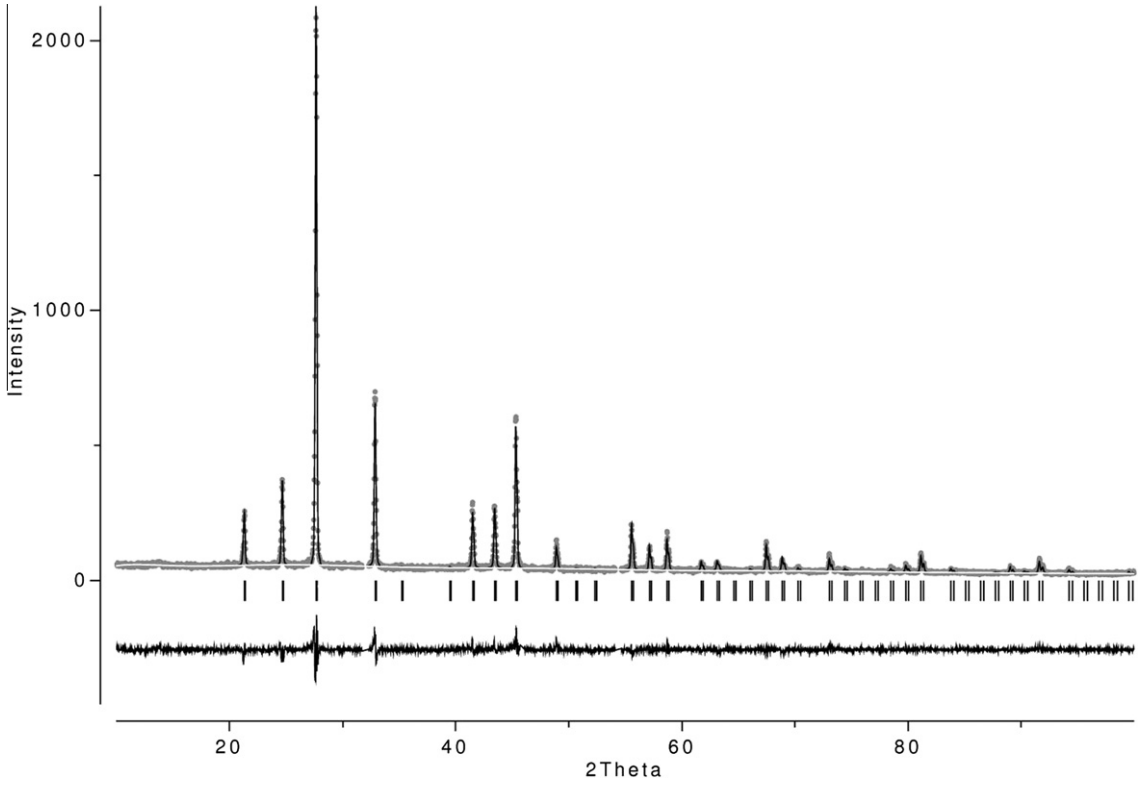

Fig. 4. Rietveld plot of observed and calculated diffraction pattern of $Sr_7Th_4(PO_4)_6$.

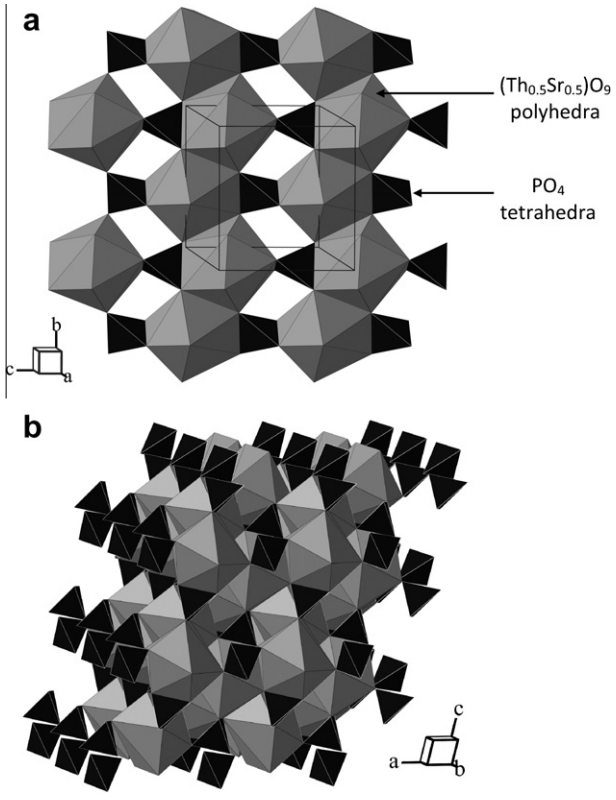

Fig. 5. (a) $[(Th_{0.5}Sr_{0.5})PO_7]_\infty$ single layer of $SrTh(PO_4)_2$; (b) typical three-dimensional structural representation of $SrTh(PO_4)_2$.

the three compounds are listed in Tables 3 and 4 respectively. The observed and calculated diffraction patterns of $SrTh(PO_4)_2$, $SrTh_4(PO_4)_6$ and $Sr_7Th(PO_4)_6$ and their difference are shown in Figs. 2–4, respectively. The indices of the intense lines are shown in the figure, pointing to their positions.

$NaTh_2(PO_4)_3$ having space group C2/*c*, $CaTh(PO_4)_2$ mineral named (cheralite) having space group P21/*n* and $Ba_3La(PO_4)_3$ having eulytite structure with space group I-43d were used as model compounds for the refinement of X-ray data of $SrTh_4(PO_4)_6$, $SrTh(PO_4)_2$ and $Sr_7Th(PO_4)_6$ compounds, respectively [51,37,52]. The structure of $SrTh(PO_4)_2$ compound is shown in Fig. 5b which is made up of $(Th,Sr)O_9$ polyhedra (Th and Sr occupying same atomic position) and PO_4 tetrahedra. The $SrTh(PO_4)_2$ structure in simple way can be described as $(Th,Sr)O_9$ polyhedra linked by edge sharing to form chain along *b*-axis direction which are linked by edge shared PO_4 tetrahedra forming layer $[(Th_{0.5}Sr_{0.5})PO_7]_\infty$ parallel to (0 1 1) plane (Fig. 5a). Each such layer is again linked to another layer along *a*-axis direction by $(Th,Sr)O_9$ polyhedra edge sharing and PO_4 tetrahedra corner sharing to complete the three-dimensional structure.

Structure of $SrTh_4(PO_4)_6$ is shown in Fig. 6b which is made of PO_4 tetrahedra and ThO_9 polyhedra sharing their apices and edges. Projection along *b*-axis direction shows that its structure is made up of $[Th_2O_6(P(2)O_4)_2]_\infty$ double layers and each such double layer is linked through $P(1)O_4$ tetrahedra by edge sharing. Each $[Th_2O_6(P(2)O_4)_2]_\infty$ double layers is made up of $[ThO_4(P(2)O_4)]_\infty$ single layer (Fig. 6a) in which ThO_9 polyhedra form chain along *c*-axis with alternate corner and edge sharing and two such chains linked by corner shared $P(2)O_4$ tetrahedra. It is seen along *c*-axis direction that Sr atom is situated in void channel formed by PO_4 tetrahedra and ThO_9 polyhedra. The $[Th_2(PO_4)_3]$ groupings in $SrTh_4(PO_4)_6$ do not differ significantly with those in other related structure in the $M^ITh_2(PO_4)_3$ series [33]. Thus, it is worth mentioning here that the difference in ionic sizes of various alkaline earth ions do not affect the overall structure.

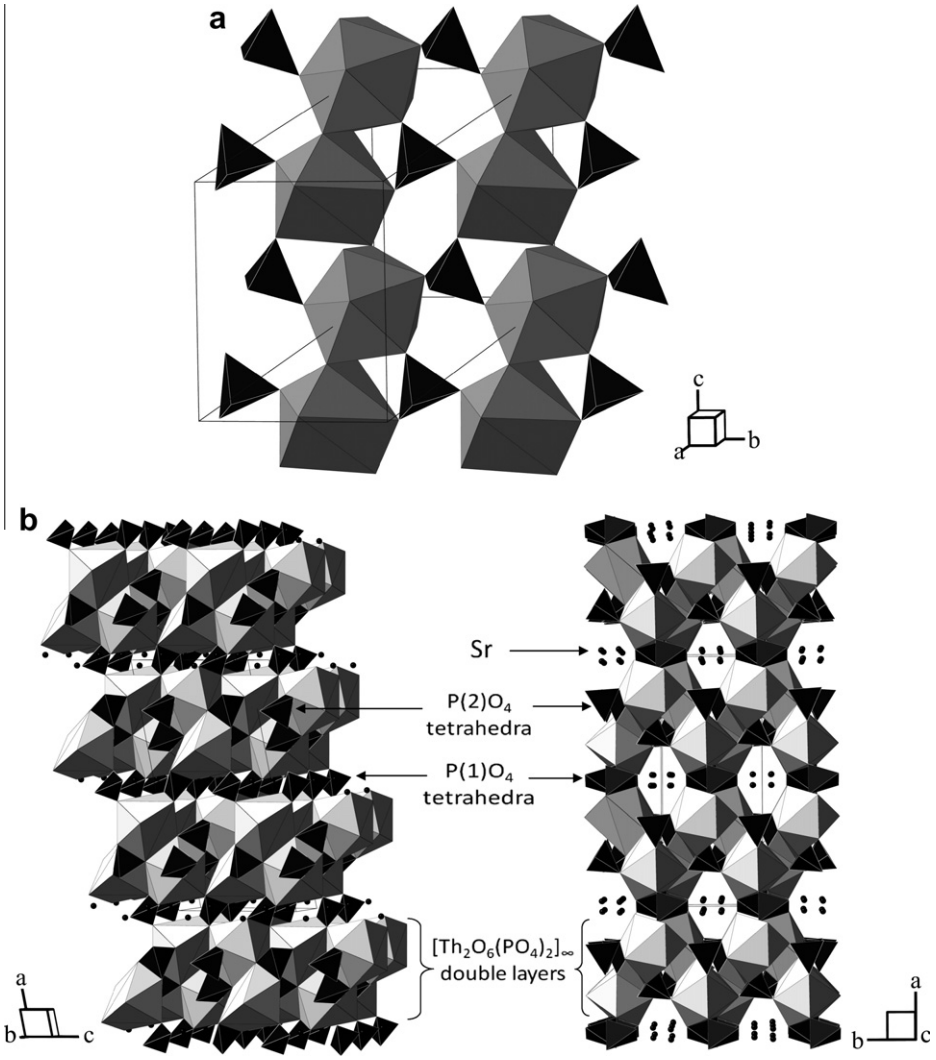

Fig. 6. (a) $[ThO_4(P(2)O_4)]_\infty$ single layer of $SrTh_4(PO_4)_6$; (b) typical three-dimensional structural representation of $SrTh_4(PO_4)_6$.

Structure of $Sr_7Th(PO_4)_6$ was refined using $Ba_3La(PO_4)_3$ structure. Such type of compounds shows cationic and oxygen sites disorders [52] and thus different models have been tried for the refinement of $Sr_7Th(PO_4)_6$ structure. It was observed that model with single oxygen site and splitted cationic site was best suited. Structure of $Sr_7Th(PO_4)_6$ is shown in Fig. 7a which is made up of Sr/Th six co-ordinate octahedral and PO_4 tetrahedra. Each PO_4 tetrahedra is connected to two pairs of four adjacent $Sr(Th)O_6$ octahedra (Fig. 7b) which is further connected to other $Sr(Th)O_6$ octahedra by edge sharing forming convoluted network.

3.3. Thermal expansion study of $SrTh(PO_4)_2$, $SrTh_4(PO_4)_6$ and $Sr_7Th(PO_4)_6$

In order to examine the thermal stability of $SrTh(PO_4)_2$, $SrTh_4(PO_4)_6$ and $Sr_7Th(PO_4)_6$ in dry air, thermograms of all the three compounds were recorded at a heating rate of 10 K min^{-1} up to 1673 K. TG curves of all the three strontium thorium phosphates did not show any weight change up to 1573 K, above which they showed slow weight loss due to decomposition of the compounds. DTA curves of the three compounds did not show any phase transition up to 1573 K. In order to find out the final decomposition products, all the three compounds were heated in a furnace at 1673 K for 24 h and the XRD patterns of the end products confirm the formation of ThO_2. Jardin et al. [53] observed decomposition of $CaTh(PO_4)_2$ under inert atmosphere above 1473 K which led to the formation of ThO_2. Though, it is reported in literature [33] that monoclinic $SrTh(PO_4)_2$ shows a phase transition at 1573 K, we could not observe any DTA peak during heating up to 1673 K.

To study the thermal expansion behavior of $SrTh(PO_4)_2$, $SrTh_4(PO_4)_6$ and $Sr_7Th(PO_4)_6$, high-temperature X-ray diffraction (HT-XRD) data of the three compounds were collected from ambient to 1273 K. It was observed that XRD patterns of all compounds remained same except shift in the X-ray line positions to lower 2θ values with increase in temperature. This indicates that the lattice parameters and cell volume of all the three compounds increases with temperature. Percentage thermal expansion of lattice parameters and cell volumes were calculated using the formula

$$\text{Expansion } (\%) = (a_T - a_{298}) \times 100/a_{298} \quad (1)$$

where a_T and a_{298} represents the lattice parameter or volume at temperature T and at 298 K, respectively.

The variation in lattice parameters a, b, c and volume (V) of monoclinic $SrTh(PO_4)_2$ and $SrTh_4(PO_4)_6$ and 'a' for cubic $Sr_7Th(PO_4)_6$ were fitted to a second order polynomial expression

$$a = x_1 + y_1T + z_1T^2 \quad (2)$$

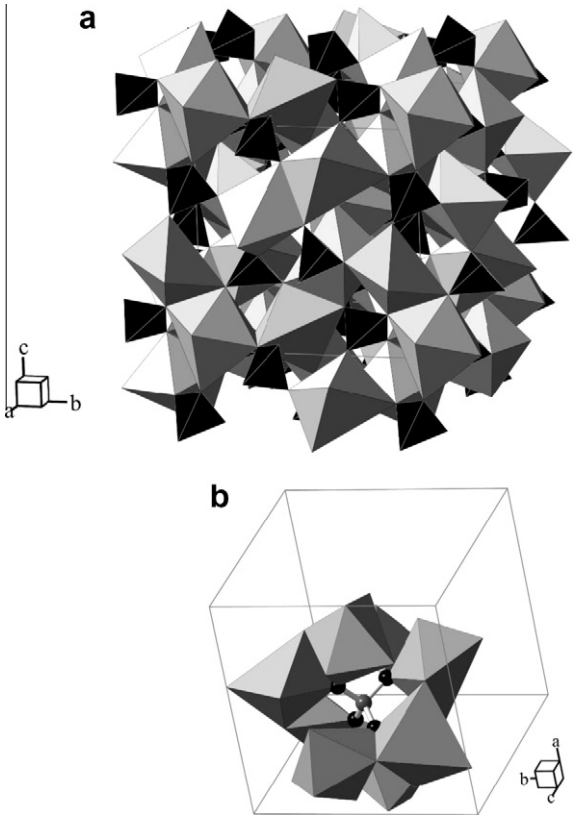

Fig. 7. (a) Typical three-dimensional structural representation of $Sr_7Th_4(PO_4)_6$; (b) PO4 tetrahedra connected to octahedra.

$$b = x_2 + y_2T + z_2T^2 \quad (3)$$

$$c = x_3 + y_3T + z_3T^2 \quad (4)$$

$$V = x_4 + y_4T + z_4T^2 \quad (5)$$

where T denotes the absolute temperature in K. The coefficients x_1, y_1 and z_1, x_2, y_2 and z_2, x_3, y_3 and z_1 and x_4, y_4 and z_4 of the fitted equations of the lattice parameters a, b, c and V, respectively against the temperature, T (K) for the three compounds are given in Table 5.

The axial (α_a) and linear expansion coefficient (α_l) were derived from the equations $\alpha_a = (\Delta a_T/a_{298}) \times (1/\Delta T)$ and $\alpha_l = (\Delta V_T/3V_{298}) \times (1/\Delta T)$, respectively [53]. Δa_T is difference in lattice parameters at temperature T and room temperature lattice parameter (a_{298}) and ΔT is corresponding temperature difference. The mean values of axial and linear thermal expansion coefficients of $SrTh(PO_4)_2$, $SrTh_4(PO_4)_6$ and $Sr_7Th(PO_4)_6$ between 298 and 1273 K are given in Table 6.

To see the effect of Sr/Th ratio on thermal expansion, the% volume expansions of $SrTh(PO_4)_2$, $SrTh_4(PO_4)_6$ and $Sr_7Th(PO_4)_6$ were plotted as a function of temperature and are shown in Fig. 8. It can be seen from the figure that% volume expansion varies linearly for all the three the compounds and remains almost same over the temperature range of investigation.

Table 6
Mean axial and linear thermal expansion coefficients of $SrTh(PO_4)_2$, $SrTh_4(PO_4)_6$ and $Sr_7Th(PO_4)_6$ between 298 and 1273 K.

Compound	Mean thermal expansion coefficient			
	Axial $10^{-6}(K^{-1})$			Linear $10^{-6}(K^{-1})$
$SrTh(PO_4)_2$	$\alpha_a = 8.77$	$\alpha_b = 10.25$	$\alpha_c = 10.95$	$\alpha_l = 8.18$
$SrTh_4(PO_4)_6$	$\alpha_a = 9.12$	$\alpha_b = 11.87$	$\alpha_c = 6.03$	$\alpha_l = 8.13$
$Sr_7Th(PO_4)_6$	$\alpha_a = 7.13$	–	–	$\alpha_l = 7.13$

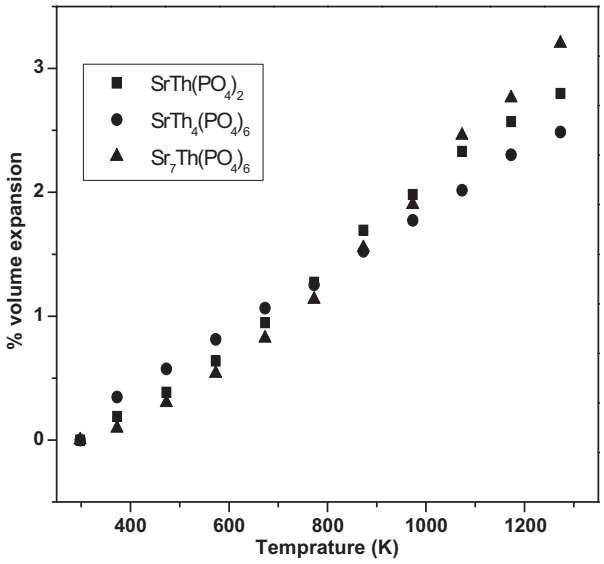

Fig. 8. Plot of% volume expansion of $SrTh_4(PO_4)_6$, $SrTh_4(PO_4)_6$ and $Sr_7Th_4(PO_4)_6$ vs temperature in the range of 298–1273 K.

4. Conclusions

Based on well established phases in SrO–ThO_2, SrO–P_2O_5 and ThO_2–P_2O_5 ternary systems and 19 phase mixtures synthesized and analyzed by XRD in the present work, a quasi ternary phase diagram of SrO–ThO_2–P_2O_5 system was drawn and three quaternary compounds, $SrTh(PO_4)_2$, $Sr_7Th(PO_4)_6$ and $SrTh_4(PO_4)_6$ were identified and their structures were determined. These compounds are stable up to 1573 K and decompose to give ThO_2 at 1673 K. HT-XRD study shows positive thermal expansion for $SrTh(PO_4)_2$, $SrTh_4(PO_4)_6$ and $Sr_7Th(PO_4)_6$ between the temperature range of 298–1273 K with mean linear expansion coefficients $\alpha_l = 8.18$, 8.13 and $7.13 \times 10^{-6}\,K^{-1}$, respectively.

Acknowledgement

The authors are thankful to Dr. S.K. Aggarwal, Head, Fuel Chemistry Division, for his keen interest and valuable suggestion in this work.

Table 5
Coefficients of the second order polynomial equations $a(x_1, y_1, z_1)$, $b(x_2, y_2, z_2)$, $c(x_3, y_3, z_3)$ and $V(x_4, y_4, z_4)$ used to fit the lattice parameters a, b, c and V against temperature, T (K) for $SrTh(PO_4)_2$, $SrTh_4(PO_4)_6$ and $Sr_7Th(PO_4)_6$.

Compound	x_1	y_1 ($\times10^{-5}$)	z_1 ($\times10^{-9}$)	x_2	y_2 ($\times10^{-5}$)	z_2 ($\times10^{-9}$)	x_3	y_3 ($\times10^{-5}$)	z_3 ($\times10^{-9}$)	x_4	y_4 ($\times10^{-5}$)	z_4 ($\times10^{-9}$)
$SrTh(PO_4)_2$	0.6775	0.98363	−1.8663	0.7003	3.5922	0.9540	0.6494	1.0028	−0.766	0.3004	0.7787	0.8672
$SrTh_4(PO_4)_6$	1.7369	1.8782	−5.0132	0.6808	1.0073	−1.4915	0.8082	0.3966	1.4452	0.9386	2.6059	−1.6957
$Sr_7Th(PO_4)_6$	1.0176	1.4933	−64.492	–	–	–	–	–	–	1.0539	0.0044	2.0492

References

[1] R.K. Sinha, A. Kakodkar, Nucl. Eng. Des. 236 (2006) 683.
[2] R. Bros, J. Carpena, V. Sere, A. Beltritti, Radiochim. Acta 74 (1996) 277.
[3] L.A. Boatner, B.C. Sales, in: W. Lutze, R.C. Ewing (Eds.), Radioactive Waste Forms for the Future, North-Holland, Amsterdam, 1988, p. 495.
[4] A. Meldrum, L.A. Boanter, W.J. Weber, R.C. Ewing, Geochim. Cosmochim. Acta 62 (1998) 2509.
[5] R. Podor, M. Cuney, Am. Miner. 82 (1997) 65.
[6] R. Podor, M. Cuney, C. Nguyen Trung, Am. Miner. 80 (1995) 1261.
[7] J.M. Montel, J.L. Devidal, D. Avignent, Chem. Geol. 191 (2002) 89.
[8] L. Bois, M.J. Guitter, F. Crrot, P. Trocellier, M. Gautier-Soyer, J. Nucl. Mater. 297 (2001) 129.
[9] H.T. Hawkins, B.E. Scheetz, G.D. Gurthrie, Chem. Mater. 11 (1999) 2851.
[10] P. Benard, V. Brandel, N. Dacheux, S. Jaulmes, S. Launay, C. Lindecker, M. Quarton, Chem. Mater. 8 (1996) 181.
[11] P.Y. Shih, Mater. Chem. Phys. 80 (2003) 299.
[12] C.W. Kim, D.E. Day, J. Non-Cryst. Solids 331 (2003) 20.
[13] N. Dacheux, N. Clavier, A.C. Robisson, O. Terra, F. Audubert, J.E. Lartigue, C. Guy, CR Chimica 7 (2004) 1141.
[14] V. Brandel, N. Dacheux, M. Genet, J. Alloys Compd. 236 (1998) 271.
[15] N. Dacheux, A.C. Thomas, V. Brandel, M. Genet, J. Nucl. Mater. 257 (1998) 108.
[16] N. Clavier, N. Dacheux, R. Podor, Inorg. Chem. 45 (2006) 220.
[17] N. Clavier, N. Dacheux, C. Wallez, M. Quarton, J. Nucl. Mater. 352 (2006) 209.
[18] S. Launay, G. Wallez, M. Quarton, Chem. Mater. 13 (2001) 2833.
[19] K.R. Laud, F.A. Hummel, J. Am. Ceram. Soc. 54 (1971) 296.
[20] V. Brandel, N. Dacheux, M. Genet, Radiochemistry 43 (2001) 6.
[21] N. Clavier, G. Wallez, N. Dacheux, D. Bregiroux, M. Quarton, P. Beaunier, J. Solid State Chem. 181 (2008) 3352.
[22] A.C. Thomas, N. Dacheux, V. Brandel, P. Le Coustumer, M. Genet, J. Nucl. Mater. 295 (2001) 249.
[23] A.C. Robisson, N. Dacheux, J. Aupiais, J. Nucl. Mater. 306 (2002) 134.
[24] A.I. Orlova, D.B. Kitaev, Radiochemisty 47 (2005) 14.
[25] V. Brandel, N. Dacheux, J. Solid State Chem. 177 (2004) 4743.
[26] V. Brandel, N. Dacheux, J. Solid State Chem. 177 (2004) 4755.
[27] V. Brandel, N. Dacheux, M. Genet, CR Chimica 5 (2002) 599.
[28] K. Krishnan, S.K. Sali, K.D. Singh Mudher, J. Alloys Compd. 414 (2006) 310.
[29] A. Guesdon, J. Provost, B. Raveau, J. Mater. Chem. 9 (1999) 2583.
[30] R.D. Purohit, A.K. Tyagi, M.D. Mathews, S. Saha, J. Nucl. Mater. 280 (2000) 51.
[31] C.E. Bamberger, R.G. Haire, G.M. Begun, H.E. Hellwege, J. Less Common Met. 102 (1984) 179.
[32] R.G. Sarawadekar, S.B. Kulkarni, Thermochim. Acta 67 (1983) 333.
[33] A.J. Locock, in: S.V. Krivovichev, P.C. Burns, I.G. Tananaev (Eds.), Structural Chemistry of Inorganic Actinide Compounds, Elsevier B.V., 2007, p. 217 (Chapter 6).
[34] PDF No. 33-1354, International Centre for Diffraction Data, Newtown Square, USA.
[35] PDF No. 35-64, International Centre for Diffraction Data, Newtown Square, USA.
[36] K. Popa, G. Wallez, P.E. Raison, D. Bregiroux, C. Apostolidis, P. Lindqvist-Reis, R.J.M. Konings, Inorg. Chem. 49 (2010) 6904.
[37] P.E. Raison, R. Jardin, D. Bregiroux, R.J.M. Konings, T. Geisler, C.C. Pavel, J. Rebizant, K. Popa, Phys. Chem. Miner. 35 (2008) 603.
[38] D. Bregiroux, O. Terra, F. Audubert, N. Dacheux, V. Serin, R. Podor, D. Bernache-Assollant, Inorg. Chem. 46 (2007) 10372.
[39] D.N. Rose, Jb. Miner. Mh. 6 (1980) 247.
[40] Meera Keskar, K. Krishnan, N.D. Dahale, J. Alloys Compd. 458 (2008) 104.
[41] R. Subasri, C. Mallika, T. Mathews, V.S. Sastry, O.M. Sridharan, J. Nucl. Mater. 312 (2003) 249.
[42] I.R. Shein, K.I. Shein, A.L. Ivanovski, J. Nucl. Mater. 361 (2007) 69.
[43] S.R. Dharwadkar, Prog. Cryst. Growth Charact. Mater. 45 (2002) 29.
[44] G. Blasse, J. Alloys Compd. 192 (1993) 17.
[45] H.A. Hoppe, Solid State Sci. 7 (2005) 1209.
[46] I.D. Brown, C. Calvo, J. Solid State Chem. 1 (1970) 173.
[47] A.A. Belik, B.I. Lazoryak, K.V. Pokholok, T.P. Terekhina, I.A. Leonidov, E.B. Mitberg, V.V. Karelina, D.G. Kellerman, J. Solid State Chem. 162 (2001) 113.
[48] Y.C. Zhang, W.D. Cheng, D.S. Wu, H. Zhang, D.G. Chen, Y.J. Gong, Z.G. Kan, J. Solid State Chem. 177 (2004) 2610.
[49] A.C. Larson, R.B. von Drecle, Los Alamos National Laboratory, LAUR-86, 2000.
[50] B.H. Toby, J. Appl. Cryst. 34 (2001) 210.
[51] B. Matkovic, B. Kojic-Prodic, M. Sljukic, M. Topic, R.D. Willett, F. Pullen, Inorg. Chim. Acta 4 (1970) 571.
[52] E.H. Arbib, B. Elouadi, J.P. Chaminade, J. Darriet, Mater. Res. Bull. 35 (2000) 761.
[53] R. Jardin, C.C. Pavel, P.E. Raison, D. Bouexiere, H. Santa-Cruz, R. J.M. Koning, K. Popa, J. Nucl. Mater. 378 (2008) 167.